Comparison of the Utility of High-Resolution CT-DWI and T2WI-DWI Fusion Images for the Localization of Cholesteatoma

X. Fan, C. Ding, and Z. Liu

ABSTRACT

BACKGROUND AND PURPOSE: Cholesteatoma is an aggressive disease that may lead to hearing impairment. This study aimed to compare the utility of high-resolution CT and TSE-DWI fusion images with that of T2WI and TSE-DWI fusion images in the localization of middle ear cholesteatoma.

MATERIALS AND METHODS: Seventy-one patients with middle ear cholesteatoma were retrospectively recruited. High-resolution CT, T2WI with fat suppression, and TSE-DWI scans were obtained, and image fusion was performed using a 3D reconstruction postprocessing workstation to form CT-DWI and T2WI-DWI fusion images. The quality of the 2 fused images was subjectively evaluated using a 5-point Likert scale with the horizontal semicircular canal transverse position as the reference. Receiver operating characteristic analysis was performed, and the diagnostic efficacies of CT-DWI and T2WI-DWI fusion images in localizing middle ear cholesteatoma were calculated.

RESULTS: The overall quality of T2WI-DWI fusion images was slightly higher than that of CT-DWI fusion images ($P < .001$), and the semicircular canal was slightly less clear on T2WI-DWI than on CT-DWI ($P < .001$). No statistical difference was found in the diagnostic confidence between them. In the localization of middle ear cholesteatoma, the accuracy, sensitivity, and specificity of T2WI-DWI fusion images and CT-DWI fusion images were equivalent for involvement of the attic, tympanic cavity, mastoid antrum, and mastoid process, with no statistically significant differences.

CONCLUSIONS: T2WI-DWI fusion images could replace CT-DWI in the preoperative selection of surgical options for middle ear cholesteatoma.

ABBREVIATION: HRCT = high-resolution CT

Cholesteatoma is an aggressive disease that can lead to conductive hearing impairment, facial palsy, labyrinthine fistula, brain abscess, and sigmoid sinus thrombosis when the lesion expands and invades adjacent structures.[1] Currently, surgical resection is the only treatment for cholesteatoma. The choice of a surgical approach varies according to the location and extent of cholesteatoma involvement;[2] therefore, precise preoperative localization is crucial.[3,4] DWI is commonly used by head and neck specialists as an imaging sequence to detect cholesteatoma,[5] especially in the diagnosis of recurrent or residual lesions.[6] Previous studies have shown that TSE-DWI has the advantages of causing fewer artifacts and providing higher lesion visibility for the diagnosis of cholesteatoma;[7] however, it is not effective in showing the landmarks of temporal bone anatomy and is not reliable for preoperative localization or determination of the surgical approach.

High-resolution CT (HRCT) is the examination of choice for cholesteatoma. This technique displays clear anatomic details of the temporal bone region. The fusion of DWI and HRCT images has been reported in previous studies[8-12] in which cholesteatoma lesions with high signal intensity on DWI were superimposed on the corresponding HRCT temporal bone structures to improve preoperative cholesteatoma detection, assessment, and localization; however, DWI and HRCT are 2 different imaging techniques, and the fusion process is cumbersome. Kanoto et al[13] and Watanabe et al[14] showed that DWI with MR cisternography can increase the accuracy of anatomic localization. However, MR cisternography sequences of the ear require additional scanning time, which may cause motion artifacts due to patient discomfort from the prolonged body position, leading to image-quality degradation.

T2WI with fat suppression is a routine MR imaging sequence that can clearly show the key anatomic landmarks of the ear in
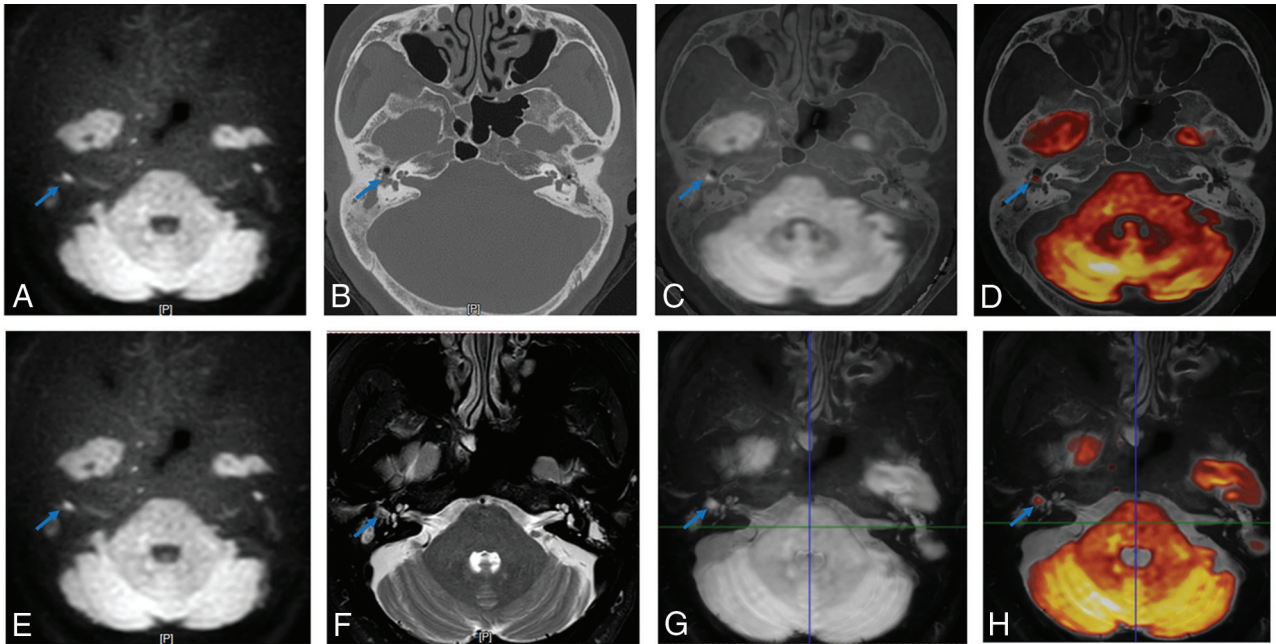
FIG 1. TSE-DWI images (*A* and *E*) were fused with HRCT (*B*) and T2WI fat-suppression images (*F*), respectively, to generate CT-DWI (*C*) and T2WI-DWI (*G*) fusion images, converting the colors to increase the visibility of the lesion (*blue arrow*) (*D* and *H*).

cholesteatoma surgery (ie, the cochlea and semicircular structures). DWI and T2WI fusion techniques are effective in localizing cholesteatoma;[15] however, they use specific T2 MR cisternography sequences instead of T2WI fat-suppression sequences in conventional ear MR imaging. Therefore, the aim of this study was to compare the image quality and localization efficacy of T2WI fat-suppression and DWI fusion images with those of HRCT and DWI fusion images in patients with middle ear cholesteatoma.

MATERIALS AND METHODS

Case Data
The clinical data of patients with initial suspicion of cholesteatoma who subsequently underwent an operation and were pathologically diagnosed as having a cholesteatoma were retrospectively collected from September 2019 to November 2021 in our otology department. Clinical data included the patient's sex and age, otoscopic findings, the presence of otopyorrhea and the odor of the secretion, and the presence of facial palsy, headache, and vertigo. The inclusion criteria for this study were the following: 1) initial clinical suspicion of cholesteatoma; 2) none of the affected ears undergoing any surgical treatment before the examination; 3) HRCT, T2WI fat-suppression sequence, and TSE-DWI examination before the operation; and 4) surgical treatment and pathologically confirmed cholesteatoma. The exclusion criteria were the following: 1) previous otologic surgery; 2) insufficient HRCT, thin-layer T2WI, or TSE-DWI image quality for image fusion; and 3) contraindication to MR imaging such as metal implants and pacemakers. This study was approved by our institutional ethics committee (2019PS069J).

Equipment and Scanning Protocol
A 256–detector row CT scanner (Philips Healthcare) was used for this study, and HRCT images were acquired with the collimation set to 20×0.625; ear HRCT scan mode (spiral sweep; pitch, 0.25; matrix, 768×768; peak, 120 kV; 200 mA/s; reconstruction layer thickness, 1 mm; interval, 0.5 mm; rotation time, 0.4 seconds; filter function, Y-Sharp [YE]; window width, 4000; window position, 700). MR imaging signals were acquired using a 3T superconducting MR imaging scanner (Ingenia; Philips Healthcare) and a 32-channel head and neck phased-array coil with the following parameters: 1) axial T2-weighted TSE and fat suppression (TR, 3000 ms; TE, 80 ms; matrix, 308×192; section thickness, 2 mm; intersection interval, 0.2 mm); and 2) axial MR imaging DWIs (b=0 and 1000 s/mm^2; TR, 3000 ms; TE, 72 ms; matrix, 118×87; section thickness, 1.5 mm; intersection interval, 1 mm). HRCT and MR imaging scans were taken from the superior edge of the petrous bone to the inferior edge of the mastoid process. All raw images were transferred in DICOM format to a 3D reconstruction postprocessing workstation (Philips) for image analysis.

Image Quality Analysis
In this study, HRCT, T2WI fat-suppression, and TSE-DWI images were jointly uploaded to the 3D reconstruction postprocessing workstation for image fusion. The fusion process was performed by experienced otolaryngologists and head and neck radiologists. HRCT, T2WI fat-suppression, and TSE-DWI were changed to the same random number code, and the HRCT was reconstructed to have the same FOV and layer thickness as the T2WI fat-suppression and TSE-DWI images. The fusion images were then automatically generated and manually fine-tuned to form CT-DWI and T2WI-DWI fusion according to the structure of the internal auditory canal and temporal bone. The fusion images were converted to color to increase the visualization of the lesion (Fig 1). Due to the high keratin content of the cholesteatoma, the temporal bone region shows marked high signal

intensity on the TSE-DWI sequence ($b=1000$ s/mm^2).[7] On the basis of these signal characteristics, the red area of the temporal bone on both fusion images was defined as a cholesteatoma, and the gray area was defined as the absence of cholesteatoma (Fig 2). Two experts independently scored the quality of both CT-DWI and T2WI-DWI fusion images subjectively, including the overall quality of fusion images, lateral semicircular canal display, lesion clarity, and diagnostic confidence. The lateral semicircular canal transverse position was used as the reference, and the 2 fusion images were scored separately using the Likert 5-point tabulation (Table 1). A score of ≥3 was considered acceptable, and the weighted κ test was performed to measure the consistency of the 2 experts' scores.

Evaluation of Efficacy in Cholesteatoma Localization

The location of the cholesteatoma was recorded in detail in all surgical patients. Patients with a subjective score of <3 for both fused images were excluded from further localization diagnosis. In this study, 4 anatomic regions of the middle ear (attic, tympanic cavity, mastoid antrum, and mastoid cavity) were used for localization as proposed by Kanoto et al:[13] 1) attic: superior to the horizontal semicircular canal and anterior to the posterior margin of the horizontal semicircular canal; 2) the tympanic cavity: inferior to the horizontal semicircular canal and anterior to the posterior margin of the horizontal semicircular canal; 3) the mastoid antrum: superior to the horizontal semicircular canal and posterior to the posterior border of the horizontal semicircular canal; and 4) mastoid cells: inferior to the horizontal semicircular canal and posterior to the posterior border of the horizontal semicircular canal.

For each lesion, 2 experienced head and neck radiologists independently evaluated the presence or absence of a cholesteatoma at each site of the temporal bone. Both specialists were blinded to the patient's surgical data and findings. The diagnostic efficacy of

FIG 2. Left middle ear mastoid region. *A*, CT-DWI fusion image of a cholesteatoma in red (*blue arrowhead*) and inflammatory tissue in gray (*green arrow*). *B*, T2WI-DWI fusion image of cholesteatoma in red (*blue arrowhead*) and inflammatory tissue in gray (*green arrow*).

the 2 fusion images for localization of the 4 anatomic regions was assessed using the intraoperative location of the cholesteatoma in the temporal bone region, which is considered the reference standard. To prevent recall bias, we assessed the 2 fusion images at 1-week intervals in a randomized order.

Statistical Analysis

All data were statistically analyzed using SPSS 22.0 (IBM) and MedCalc statistical software, Version 19.6 (MedCalc Software). After we tested for normality, data conforming to a normal distribution were expressed as mean (SD), and comparisons were performed using an independent samples t test; $P < .05$ was considered statistically significant. Two experts were used for the statistical analysis of the diagnostic agreement of the fused graphs, using the weighted κ test. The weighted κ coefficients were defined as follows: poor (0.00–0.30), fair (0.31–0.50), moderate (0.51–0.70), good (0.71–0.90), and excellent (0.91–1.00). The Wilcoxon rank-sum test was used to compare the overall quality scores of CT-DWI and T2WI-DWI fusion images. The accuracy, sensitivity, and specificity of CT-DWI and T2WI-DWI fusion image data were calculated, and the diagnostic efficacy of the 2 fusion images was compared by receiver operating characteristic analysis.

RESULTS

Basic Patient Information

All 106 patients with initial clinical suspicion of cholesteatoma underwent an operation, including 75 patients with pathologically confirmed cholesteatoma, of which 4 cases were excluded due to image artifacts in TSE-DWI, T2WI, and HRCT. A total of 71 patients were included. The mean interval between CT and MR imaging in these patients was 2.08 (SD, 3.47) days, with the shortest interval being 0 days and the longest interval being 23 days. The mean interval between MR imaging and an operation was 4.77 (SD, 3.36) days, with a minimum interval of 1 day and a maximum interval of 18 days. The measured mean lesion diameter in the cholesteatoma group was 10.17 (SD, 6.51) mm (range, 2.0–35.0 mm).

Subjective Evaluation of CT-DWI and T2WI-DWI Fusion Images

The subjective evaluation of fusion image quality by the 2 experts was consistent, with κ values of >0.80 (Table 2). Although the overall quality of both CT-DWI and T2WI-DWI fusion images was higher (Fig 3*A*), the overall quality of CT-DWI fusion images was slightly lower than that of T2WI-DWI ($P < .001$). Both experts were well able to distinguish the landmark anatomic structures of the middle ear region on CT-DWI and T2WI-DWI. Using the horizontal semicircular canal as a reference, both experts could clearly distinguish the anterior and posterior branch margins of the horizontal semicircular canal in the transverse position on the fusion images (Fig 3*B*); however, the score of the clarity of the
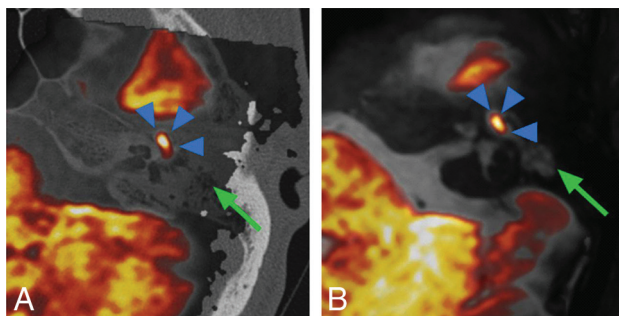
Table 1: Subjective evaluation of fusion image quality

Score	Overall Quality of the Fusion Image	Semicircular Canal Display	Clarity of the Lesion	Diagnostic Confidence
1	Unacceptable	Difficult to identify edges	Severe blurring of contours	Very poor
2	Poor, evaluation moderately limited	Blurred edges, but identifiable	Blurred contours	Poor
3	Moderate, evaluation mildly limited	Margins recognizable	Contours recognizable	Moderate
4	Good, evaluation less limited	Edges visible, no distortion	Contour edges visible	Good
5	Very good	Clear edges	Clear contours	Very good

semicircular canal display was slightly higher on CT-DWI than on T2WI-DWI ($P < .001$). Both CT-DWI and T2WI-DWI fusion images had higher subjective scores for lesion significance and diagnostic confidence of cholesteatoma localization in the middle ear mastoid (Fig 3C, -D) without statistical differences (lesion significance, $P = .62$; diagnostic confidence, $P = .59$). However, in 10 cases, the outline of the red portion in the temporal bone region on both fusion images was blurred due to small cholesteatoma size, with a score of <3.

Evaluation of the Diagnostic Efficacy of Cholesteatoma Localization

Patients with cholesteatomas with 2 fusion scores of <3 were excluded, and 61 patients with cholesteatomas were finally included for the localization of 4 key anatomic landmarks in the middle ear. CT-DWI and T2WI-DWI fusion images showed no statistical difference in area under the curve for the 4 anatomic regions, as detailed in Table 3. Except for the tympanic cavity, the accuracy of T2WI-DWI fusion images for localization of the attic,

tympanic sinus, and mastoid process was slightly higher than that of CT-DWI fusion images (Figs 4 and 5).

DISCUSSION

The results of this study showed that the T2WI-DWI fusion produced images of good overall quality, with high sensitivity, specificity, and accuracy for landmark localization of cholesteatoma, without substantial differences from CT-DWI fusion images, therefore meeting the requirements for preoperative surgical evaluation and selection of the surgical approach.

It has been demonstrated that CT-DWI fusion images improve the accuracy of the preoperative diagnosis of cholesteatoma by combining the diagnostic ability of DWI with the localization capacity of CT.[8,9,11] In this study, the overall image quality of T2WI-DWI fusion images was higher than that of CT-DWI fusion images. This is likely due to the interval between the preoperative CT and DWI examinations and the continuous growth of the cholesteatoma, resulting in imprecise matching of the lesion displayed in the 2 images. T2WI-DWI fusion images can well avoid the problem of temporal inconsistency between the 2 images. These images are based on 2 sequences from the same MR imaging scan using the same machine and scan position, thus shortening the processing time for image fusion and reducing manual alignment bias caused by the fusion of images from both CT and DWI techniques. Moreover, MR imaging fusion

Table 2: Comparison of subjective evaluation agreement between CT-DWI and T2WI-DWI fusion images[a]

	CT-DWI, Interobserver κ (95% CI)	T2WI-DWI, Interobserver κ (95% CI)
Overall quality of fusion image	0.82 (0.71–0.93)	0.87 (0.73–1.00)
Semicircular canal display	0.88 (0.77–0.98)	0.81 (0.70–0.92)
Clarity of the lesion	0.94 (0.88–0.99)	0.93 (0.88–0.99)
Diagnostic confidence	0.93 (0.86–0.99)	0.91 (0.85–0.97)

[a] κ indicates weighted κ coefficients.
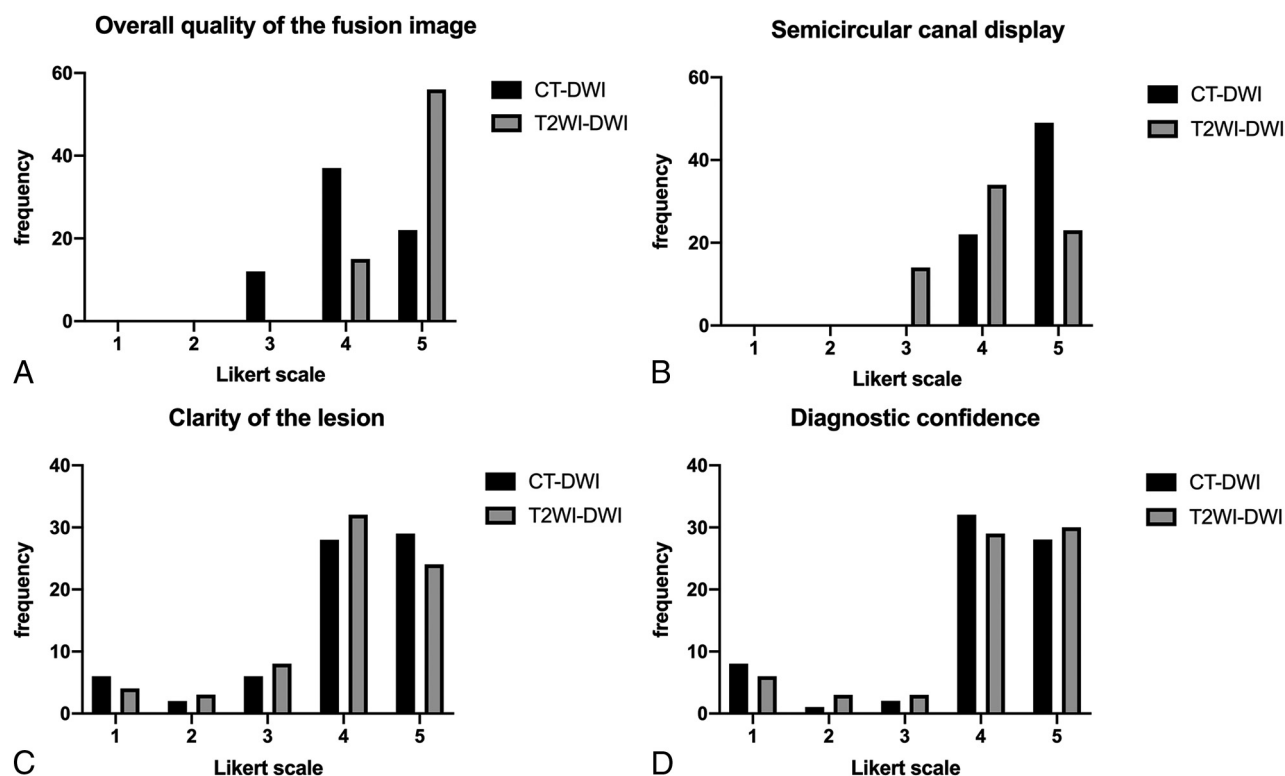

FIG 3. Subjective evaluation of CT-DWI and T2WI fusion image quality.

Table 3: Diagnostic efficacy of middle ear mastoid localization in CT-DWI fusion and T2WI-DWI fusion images

	Sensitivity	Specificity	AUC	AUC 95% CI	P Value
Attic					.32
CT-DWI	0.98	0.75	0.87	0.76–0.94	
T2WI-DWI	1.00	0.75	0.88	0.77–0.95	
Tympanic cavity					.30
CT-DWI	0.84	0.86	0.85	0.74–0.93	
T2WI-DWI	0.84	0.72	0.78	0.66–0.88	
Mastoid antrum					.70
CT-DWI	0.76	0.87	0.82	0.70–0.90	
T2WI-DWI	0.79	0.87	0.83	0.71–0.91	
Mastoid cavity					.16
CT-DWI	0.75	0.85	0.80	0.68–0.89	
T2WI-DWI	0.82	0.82	0.85	0.74–0.93	

Note:—AUC indicates area under the curve.
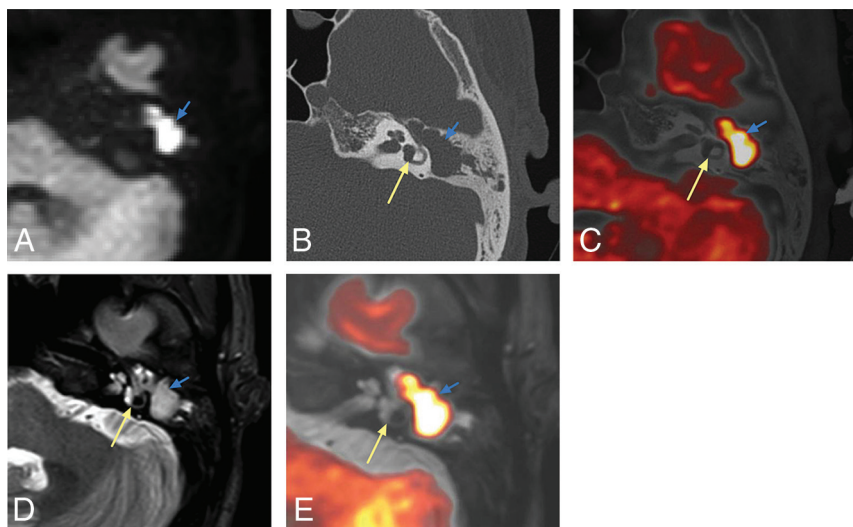
FIG 4. Pathologically confirmed cholesteatoma. The attic and mastoid antrum are filled with cholesteatoma during the operation. *A*, TSE-DWI: a high signal intensity area (*blue arrow*) is seen in the mastoid of the left middle ear with clear borders and poorly displayed semicircular canal. *B*, HRCT: a soft-tissue density shadow is seen within the middle ear mastoid cavity (*blue arrow*), and the anterior and posterior pedicles of the horizontal semicircular canal are clearly displayed (*yellow arrow*). CT-DWI fusion image (*C*) shows the cholesteatoma exceeding the posterior branch of the horizontal semicircular canal, involving the mastoid antrum. *D*, T2WI shows a non-specific high-intensity-signal shadow in the mastoid process of the left middle ear. *E*, T2WI-DWI: the horizontal semicircular canal is clear, the cholesteatoma shows yellow changes, and the lesion involves the attic and mastoid antrum.

images do not pose the same ionizing radiation hazard as CT examinations, which makes them applicable to a wider range of people.

TSE-DWI and its corresponding T2WI fusion images can clearly show important anatomic landmarks, such as the lateral semicircular canal and the cochlea. Although T2WI is not sufficient to match the CT display of fine anatomy and cholesteatoma bone erosion,[16] the horizontal semicircular canal display and the relationship between the lesion and the horizontal semicircular canal are the otologist's main concern because they influence the choice of the surgical approach. When the cholesteatoma lesion is confined to the attic or tympanic cavity and does not extend to the posterior limb of the lateral semicircular canal, it is resected using only the transcanal endoscopic approach; involvement of the mastoid antrum or mastoid process requires conversion to mastoidectomy (microscopic ear surgery) or the combined microscopic and endoscopic approach to resect the lesion.[17-21] Although the semicircular canal was scored slightly lower in the T2WI-DWI fusion images than in the CT-DWI fusion images, there was no statistical difference between the 2 in terms of the clarity of the cholesteatoma margins and diagnostic confidence. The sensitivity and accuracy of T2WI-DWI fusion images for involvement of the mastoid antrum and mastoid were slightly higher than those of CT-DWI fusion images in this study, though there was no statistical difference between them.

Compared with T2WI-DWI, CT-DWI had higher image resolution and more clearly showed the fine structures; however, it did not improve the ability to detect cholesteatoma involvement of the mastoid antrum and mastoid cavity. Therefore, T2WI-DWI fusion images can competently assess whether the mastoid antrum and mastoid process are preoperatively involved. The diagnostic accuracy of the present study for mastoid antrum involvement (83%) was slightly lower than that of the study by Benson et al[15] (93.3%), probably due to the thicker layer (2 mm) of the T2WI fat-suppression sequence routinely used in the present study. Benson et al[15] used a thinner layer (0.6 mm) with the T2 sampling perfection with application-optimized contrasts by using different flip angle evolution (SPACE sequence; Siemens) technique, and the thinner scan thickness allowed a clearer display of the cholesteatoma border. The sensitivity and specificity for the mastoid region in this study was slightly lower than those reported in other studies,[17] probably due to the absence of a combined T1WI sequence to exclude cholesterol granulomas.

The accuracy of T2WI-DWI fusion images in this study was slightly superior to that of CT-DWI for localization of the attic. This is probably because the cholesteatoma lesion was smaller, and a large amount of inflammatory tissue surrounding the lesion showed a substantially high intensity signal in the TSE-DWI sequence, thus obscuring the location of the red lesion in the CT-DWI fusion images. In contrast, the inflammatory tissue showed high signal intensity on the T2WI suppressed images, which were fused with the DWI, giving rise to complete T2WI-DWI images for the evaluation of the cholesteatoma. The accuracy of CT-DWI and T2WI-DWI fusion images for attic localization in this
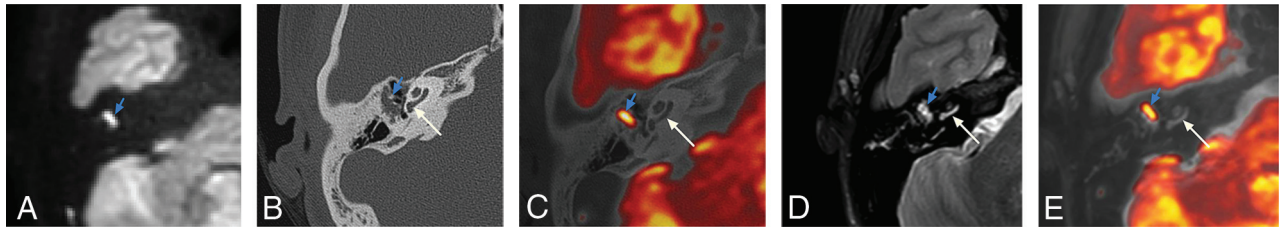
FIG 5. Surgical confirmation of a cholesteatoma in the tympanic cavity. *A*, TSE-DWI: a clear high-intensity-signal area (*blue arrow*) with a clear border in the right middle ear. *B*, HRCT: soft-tissue density shadow (*blue arrow*) in the middle ear with an unclear border and clear cochlear structures (*yellow arrows*). CT-DWI fusion image (*C*) clearly shows the cholesteatoma in the tympanic cavity. *D*, T2WI shows a nonspecific high-intensity-signal shadow in the mastoid process of the right middle ear. *E*, T2WI-DWI shows a clear cochlea with the cholesteatoma, localized in the tympanic cavity with reddish-yellow changes.

study was slightly higher than that reported by Felici et al.[11] This difference is probably because our study included only unoperated patients, whereas Felici et al[11] included patients with postoperative recurrence of cholesteatoma. In such patients, the structures were relatively less easy to identify, which is also consistent with the results of Benson et al.[15] When the cholesteatoma is located in the tympanic cavity, the diagnostic yield of T2WI-DWI fusion images is slightly lower than that of CT-DWI fusion images. This may be because CT-DWI images can clearly distinguish the boundary between the external auditory canal and the tympanic cavity, whereas T2WI-DWI cannot, easily leading to the confusion of lesions within the external auditory canal with lesions in the tympanic cavity.

This study has the following shortcomings and limitations. First, all included patients had surgically and pathologically confirmed cholesteatoma, and only the localization accuracy for cholesteatoma was evaluated; the diagnostic efficacies of the 2 fusion techniques for cholesteatoma were not compared. Second, only patients with an initial cholesteatoma were included to evaluate whether T2WI-DWI can replace CT-DWI as the procedure of choice for patients with cholesteatomas, and the localization of lesions in patients with recurrent disease has not been evaluated. Numerous studies have shown that DWI sequences can replace secondary surgical exploration to evaluate patients for cholesteatoma recurrence.[6] Whether T2WI-DWI fusion images can be used to guide the surgical options in patients with suspected recurrence is a prospective topic for future research. Third, image fusion is postprocessed on a separate workstation with more workflow; however, many PACS vendors are beginning to incorporate autoregistration and image fusion into their postprocessing functions, which can minimize procedural errors during image transfer and reduce reliance on third-party applications.[22,23] As PACS advanced postprocessing functions become more sophisticated, image-fusion techniques will become an efficient workflow and gain wider adoption. Finally, T1WI sequences have great advantages for excluding cholesterol granuloma,[17] and T1WI sequences may be added in future studies for synergistic diagnosis[24,25] to reduce false-positive rates.

CONCLUSIONS

In this study, we compared T2WI-DWI fusion images with CT-DWI fusion images in terms of image quality and localization of middle ear cholesteatoma. The T2WI-DWI fusion image can

clearly assess the involvement of cholesteatoma on the attic, tympanic cavity, mastoid antrum, and mastoid process, which can assist clinicians in the preoperative assessment and in the selection of the best surgical plan and optimal surgical approach. In the past, otologists could only choose the plan preoperatively on the basis of HRCT imaging and surgical experience; the choice, to a certain extent, could cause subjective bias. The development of T2WI-DWI fusion imaging can provide technical support for cholesteatoma diagnosis and operative treatment.

Disclosure forms provided by the authors are available with the full text and PDF of this article at www.ajnr.org.

REFERENCES

1. Yung M, Tono T, Olszewska E, et al. **EAONO/JOS Joint Consensus Statements on the Definitions, Classification and Staging of Middle Ear Cholesteatoma.** *J Int Adv Otol* 2017;13:1–8 CrossRef Medline
2. Chiao W, Chieffe D, Fina M. **Endoscopic management of primary acquired cholesteatoma.** *Otolaryngol Clin North Am* 2021;54:129–45 CrossRef Medline
3. Anschuetz L, Presutti L, Marchioni D, et al. **Discovering middle ear anatomy by transcanal endoscopic ear surgery: a dissection manual.** *J Vis Exp* 2018;56390 CrossRef Medline
4. Prasad SC, Piras G, Piccirillo E, et al. **Surgical strategy and facial nerve outcomes in petrous bone cholesteatoma.** *Audiol Neurootol* 2016;21:275–85 CrossRef Medline
5. Lingam R, Bassett P. **A meta-analysis on the diagnostic performance of non-echoplanar diffusion-weighted imaging in detecting middle ear cholesteatoma: 10 years on.** *Otol Neurotol* 2017;38:521–28 CrossRef Medline
6. Muzaffar J, Metcalfe C, Colley S, et al. **Diffusion-weighted magnetic resonance imaging for residual and recurrent cholesteatoma: a systematic review and meta-analysis.** *Clin Otolaryngol* 2017;42:536–43 CrossRef Medline
7. Wiesmueller M, Wuest W, May MS, et al. **Comparison of readout-segmented echo-planar imaging and single-shot TSE DWI for cholesteatoma diagnostics.** *AJNR Am J Neuroradiol Neuroradiol* 2021;42:1305–12 CrossRef Medline
8. Alzahrani M, Alhazmi R, Belair M, et al. **Postoperative diffusion weighted MRI and preoperative CT scan fusion for residual cholesteatoma localization.** *Int J Pediatr Otorhinolaryngol* 2016;90:259–63 CrossRef Medline
9. Locketz GD, Li PM, Fischbein NJ, et al. **Fusion of computed tomography and PROPELLER diffusion-weighted magnetic resonance imaging for the detection and localization of middle ear cholesteatoma.** *JAMA Otolaryngol Head Neck Surg* 2016;142:947–53 CrossRef Medline
10. Campos A, Mata F, Reboll R, et al. **Computed tomography and magnetic resonance fusion imaging in cholesteatoma preoperative assessment.** *Eur Arch Otorhinolaryngol* 2017;274:1405–11 CrossRef Medline

11. Felici F, Scemama U, Bendahan D, et al. **Improved assessment of middle ear recurrent cholesteatomas using a fusion of conventional CT and non-EPI-DWI MRI.** *AJNR Am J Neuroradiol* 2019;40:1546–51 CrossRef Medline

12. Yamashita K, Hiwatashi A, Togao O, et al. **High-resolution three-dimensional diffusion-weighted MRI/CT image data fusion for cholesteatoma surgical planning: a feasibility study.** *Eur Arch Otorhinolaryngol* 2015;272:3821–24 CrossRef Medline

13. Kanoto M, Sugai Y, Hosoya T, et al. **Detectability and anatomical correlation of middle ear cholesteatoma using fused thin slice non-echo planar imaging diffusion-weighted image and magnetic resonance cisternography (FTS-nEPID).** *Magn Reson Imaging* 2015;33:1253–57 CrossRef Medline

14. Watanabe T, Ito T, Furukawa T, et al. **The efficacy of color mapped fusion images in the diagnosis and treatment of cholesteatoma using transcanal endoscopic ear surgery.** *Otol Neurotol* 2015;36:763–68 CrossRef Medline

15. Benson JC, Carlson ML, Yin L, et al. **Cholesteatoma localization using fused diffusion-weighted images and thin-slice T2 weighted images.** *Laryngoscope* 2021;131:E1662–67 CrossRef Medline

16. Cavaliere M, Di Lullo AM, Russo C, et al. **Computed-tomography-structured reporting in middle ear opacification: surgical results and clinical considerations from a large retrospective analysis.** *Front Neurol* 2021;12:615356 CrossRef Medline

17. Baba A, Kurihara S, Fukuda T, et al. **Non-echoplanar diffusion weighed imaging and T1-weighted imaging for cholesteatoma mastoid extension.** *Auris Nasus Larynx* 2021;48:846–51 CrossRef Medline

18. Migirov L, Wolf M, Greenberg G, et al. **Non-EPI DW MRI in planning the surgical approach to primary and recurrent cholesteatoma.** *Otol Neurotol* 2014;35:121–25 CrossRef Medline

19. Abdul-Aziz D, Kozin ED, Lin BM, et al. **Temporal bone computed tomography findings associated with feasibility of endoscopic ear surgery.** *Am J Otolaryngol* 2017;38:698–703 CrossRef Medline

20. Tolisano AM, Killeen DE, Hunter JB, et al. **The Antrum-Malleus-Tegmen score: a pilot study assessing preoperative radiographic predictors for transcanal endoscopic cholesteatoma dissection.** *Otol Neurotol* 2019;40:e901–08 CrossRef Medline

21. Das A, Mitra S, Ghosh D, et al. **Endoscopic versus microscopic management of attic cholesteatoma: a randomized controlled trial.** *Laryngoscope* 2020;130:2461–66 CrossRef Medline

22. Colleran GC, Kwatra N, Oberg L, et al. **How we read pediatric PET/CT: indications and strategies for image acquisition, interpretation and reporting.** *Cancer Imaging* 2017;17:28 CrossRef Medline

23. Berkowitz SJ, Wei JL, Halabi S. **Migrating to the modern PACS: challenges and opportunities.** *Radiographics* 2018;38:1761–72 CrossRef Medline

24. Fukuda A, Morita S, Harada T, et al. **Value of T1-weighted magnetic resonance imaging in cholesteatoma detection.** *Otol Neurotol* 2017;38:1440–44 CrossRef Medline

25. Moustin D, Veillon F, Karch-Georges A, et al. **Importance of signal intensity on T1-weighted spin-echo sequence for the diagnosis of chronic cholesteatomatous otitis.** *Eur Arch Otorhinolaryngol* 2020;277:1601–08 CrossRef Medline